



XIX ANIDIS Conference, Seismic Engineering in Italy

Settlement of masonry barrel vaults: an experimental and numerical study

Vieri Cardinali^{a*}, Barbara Pintucchi^b, Marco Tanganelli^a, Francesco Trovatelli^a

^aDepartment of Architecture, Piazza Brunelleschi n. 6, Florence 50121, Italy

^bDepartment of Environmental Engineering, Via di Santa Marta n. 3, Florence 50139, Italy

Abstract

The paper deals with a experimental and numerical study of a masonry barrel vault subjected to an incremental horizontal settlement of one abutment. The analyzed vault is very slender and with no backfill, as is typical of the vaulted roofs covering many Italian churches and other religious buildings of various dimensions, that often suffer a certain amount of settlement due to the deformation of the sustaining walls. In this paper, the experimental tests conducted at the University of Florence on a full-scale specimen has been assumed as a benchmark for numerical simulations carried out via different models, some implemented in the general purpose FEM software (Abaqus), and others specifically developed for masonry structures (Mady). The capability of the considered models to describe the actual behavior of the vault has been investigated, and their potential highlighted.

© 2023 The Authors. Published by Elsevier B.V.

This is an open access article under the CC BY-NC-ND license (<https://creativecommons.org/licenses/by-nc-nd/4.0>)

Peer-review under responsibility of the scientific committee of the XIX ANIDIS Conference, Seismic Engineering in Italy.

Keywords: barrel vault; laboratory test; full-scale specimen; numerical modeling; FEM

1. Introduction

Masonry structures, as they constitute a significant part of the existing urban stock, require specific attentions. Within them, the majority of constructions are dated back in the centuries, hence, they have been built following empirical rules without building codes or seismic assessment. Arches, vaults and domes are part of the most magnificent masonry constructions. The variability of solutions that can be found across the territories points out the

*Corresponding author. Tel.: +39 055 275 5410; fax: +39-055 275 5355.

E-mail address: vieri.cardinali@unifi.it

feasibility of these constructions to cover several architectural spaces. Nonetheless, as these structures are stable due to equilibrium conditions and the action of gravity force, they are also vulnerable towards settlements of their supports, horizontal forces, variations in the static schemes. In order to guarantee the safeguard of these structures, reliable constitutive models need to be defined, i) to properly represent the real conditions of the structures; ii) to propose suitable strengthening solutions. In the present paper, a study conducted on a full-scale specimen represented a portion of a barrel vault is presented. The specimen was made in the Laboratory according to a geometry which is common in churches and other buildings. The numerical analyses have been carried out adopting various finite-element models with two distinct constitutive laws. The accuracy of each strategy has been evaluated according to different dimensional analysis by executing 1-d (beam models), 2-d (plate models) and 3-d models (bricks). The comparison of the different modeling strategies has allowed to highlight their coherency with the experimental results, providing indications for suitable and parsimonious approaches in the numerical evaluations of these structural typologies.

2. Experimental test

The results provided in the following refer to the masonry vault, tested in the Laboratorio Ufficiale Prove Materiali e Strutture at the University of Florence. To summarize, the specimen consists of a full-scale deep arch representing a portion of a barrel vault, made up with UNI clay bricks (5.5x12x25 cm) and hydraulic mortar (mortar joints with a thickness of 1 cm), as shown in Fig. 1a. The geometry of the arch is represented in Fig. 1b, together with the test setup and the position of such transducers (indicated by the black dots by CPL, CP0 and CPR respectively) that provide the measures of displacements used for comparison in numerical simulations.

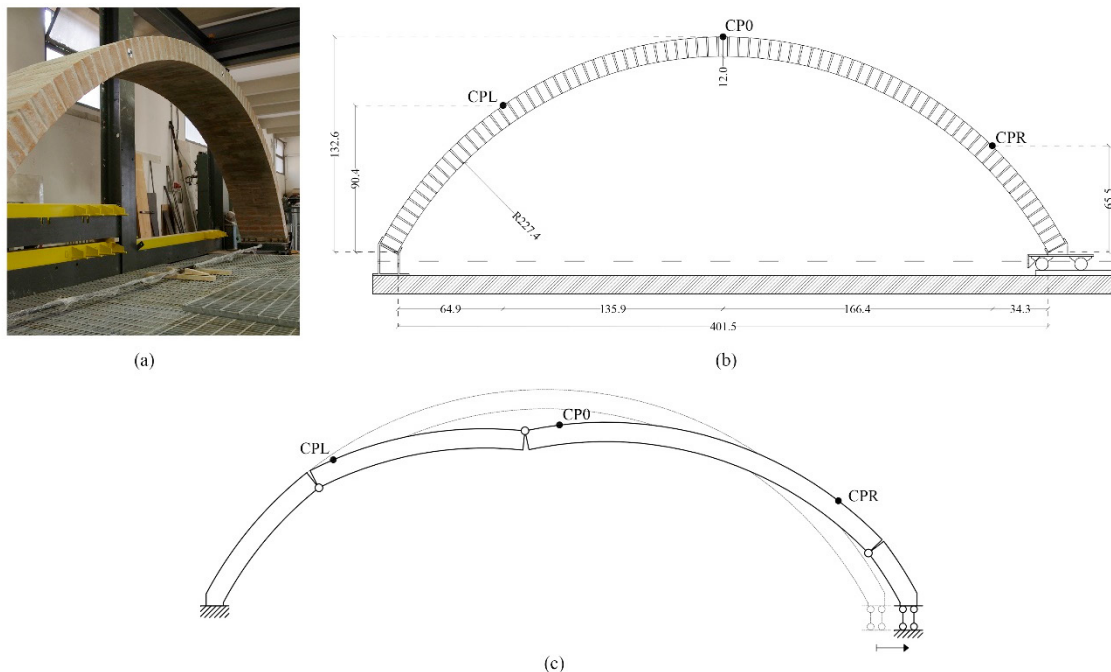


Fig. 1. (a) picture of the specimen; b) geometry of the specimen and test setup; c) final configuration of the experimental test with the formation of the three hinges.

The portion of vault was built on a fixed support on the left, and on a sliding support specifically designed to produce the horizontal settlement on the right. During the test, upon reaching the settlement of 2.5 mm, the arch began to crack on the intrados near the crown, while a second crack occurred on the extrados at the left haunch of the structure upon reaching the settlement of 7.5mm. Lastly, after the settling displacement have reached the value of 15 mm, the

last crack appears at the extrados on the right haunch, and the structure does evidence the expected mechanism with the formation of three hinges (Como, 2013). A sketch of the obtained static mechanism is shown in Fig. 1c.

Preliminarily to the experimental investigation, a series of laboratory tests were executed in order to determine the mechanical properties of the adopted masonry. In Tab. 1 the values of the mechanical parameters that have been used in the following numerical analyses are listed. They have been obtained from the experimental tests executed by compression test on 3 masonry panels of 50 x 50 cm referring to UNI EN–1052-1 with the exception of the Poisson's ratio, which has been determined on expert's judgment. Besides the mechanical parameters given in Tab. 1, values of other parameters needed to define the nonlinear behaviour of each numerical model are specifically provided in the following section together with the description of the implemented constitutive laws.

Table 1. Values of the mechanical properties adopted.

Material's properties	
Elastic Young's Modulus [MPa]	3530
Poisson's ratio ν [-]	0.2
Compressive strength [MPa]	8.8
Specific weight [kN/m ³]	17.5

3. Numerical models

Several numerical simulations of the executed experimental tests are presented. Two distinct finite-element modeling approaches have been adopted, i.e. the Mady code (Lucchesi et al. 2018a) and the commercial Abaqus (ABAQUS, 2018). Although the anisotropy of the masonry material, it has been modelled as a homogeneous continuum, as widely used in literature (D'Altri et al. 2020). The study has been developed by adopting three different modeling strategies of increasing complexity, i.e. 1-d beam models (BE), 2-d plane-stress and plates models (PL), and 3-d brick models (BR). In all models, the degrees of freedom of the supports of the vault have been fixed except for the lateral displacement in x direction of the right support, in accordance with the evidence of the experimental test. Table 2 summarizes the denominations of the analyzed numerical models. The initial letter of the acronym is referred to the adopted software (M for Mady and A for Abaqus). In addition, for the considered 2-d models a further distinction was made with respect to the assumed tensile strength. Since no specific tests were executed during the experimental campaign to determine the tensile capacity of the masonry, two different strategies have been assumed, considering: *i*) a no-tension or *quasi*-no tension behavior and *ii*) assuming a tensile strength f_t equal to the 5% of the compressive one ($f_t = 0.44$ MPa), indicated by the letter T.

Table 2. Numerical models adopted.

		1-d	2-d	3-d
Mady	No-tension	M-BE	M-PL	M-BR
	Tens. Str. = 0.44MPa		M-PLT	
Abaqus	Quasi no-tension	A-BE	A-PL	A-BR
	Tens. Str. = 0.44MPa		A-PLT	

3.1. Finite-element modeling and constitutive laws in the Mady code

The Mady models used in the numerical simulations have all been developed on purpose for masonry structures, according to an homogeneous approach. They have different levels of complexity and different constitutive hypothesis.

The simpler beam model (M-BE) is made of 180 straight finite beam elements, with three DOF for node: axial and transverse displacements, and rotation. Hermite shape functions are used in the flexural problem, while linear

functions are adopted for axial displacements (Lucchesi and Pintucchi, 2007). The model has a rectangular cross-section and is made of no-tension material with a limited compressive strength. The assumed constitutive equation given in terms of generalized stress (normal force N and bending moment M) as a function of the generalized strain (extensional strain ϵ and change of curvature κ of the beam's axis), was determined under the Euler-Bernoulli hypothesis, considering only the axial stress component σ , as detailed in (Zani, 2004, Pintucchi and Zani, 2009). Despite its simplicity, the model has evidenced a good capability to predict the response of masonry arches and other slender structures (Pintucchi and Zani, 2016, Girardi et al. 2012). In particular, the model provides some results such as the line of thrust or the amount of cracked cross-sectional area, that give quick indication on the damage state and on failure mechanisms of vaulted structures.

The more complete 2D and 3D models make all use of a constitutive equation defined for continuous bodies by assuming a constrain on the stress. This constraint implies that the stress belongs to a stress range K a closed and convex subset of the space of the second-order symmetric tensors, given by the intersection between some convex cones, each of which expressing a possible bound to the material's tensile and/or compressive and/or shear strength. Given K and the tensor C of the elastic modules, once a strain E has been assigned, the stress T is obtained by projecting CE onto K with respect to a suitably defined inner product. The strain is thus additively divided into an elastic part E_e on which T depends linearly, and into an inelastic part E_a which is characterized by belonging to the normal cone of K at T . The anelastic deformation E_a can be an indicator of the damage location throughout the structure (Lucchesi et al., 2021).

The 2D models, (M-PL and M-PLT), are made of 640 two-dimensional four-node isoparametric plane-stress elements; the M-PL uses the classical masonry-like material constitutive law, i.e., a material with null tensile strength, with a further limit to the compressive strength, defined in the framework of plane stress hypothesis (Lucchesi et al., 2018a). The M-PLT follows the same constitutive law with a limited tensile capacity.

Lastly, the 3D model, made of 3200 eight-node isoparametric brick elements (M-BR), uses the same constitutive assumption of the M-PL in its most general 3D formulation (Lucchesi et al., 2018b).

3.2. Finite-element modeling and constitutive laws in Abaqus

The three models developed through Mady software has been carried out with the same modeling strategies in Abaqus environment (Abaqus, 2018): the simplified beam model (A-BE) consist of 180 B21 elements, the 2D plane model (A-PL) of 672 S4 elements; and the 3D model (A-BR) is made of 11832 C3D8 elements.

The masonry material has been described by an elastic behaviour driven by Elastic modulus and stiffness, then the achievement of determined stress levels activates the nonlinear phase. The latter has been represented through the concrete damaged plasticity model (CDP). This material model, initially designed to describe the non-linear behavior of concrete (Lubliner et al., 1989), is widely adopted in literature to represent the masonry behavior (Scacco et al., 2020, Milani et al., 2019). The CDP is based on an isotropic material with a plasticity-damage relation that allows assigning distinct tensile and compressive strength and different post peak behaviors with damage parameters (Figure 2).

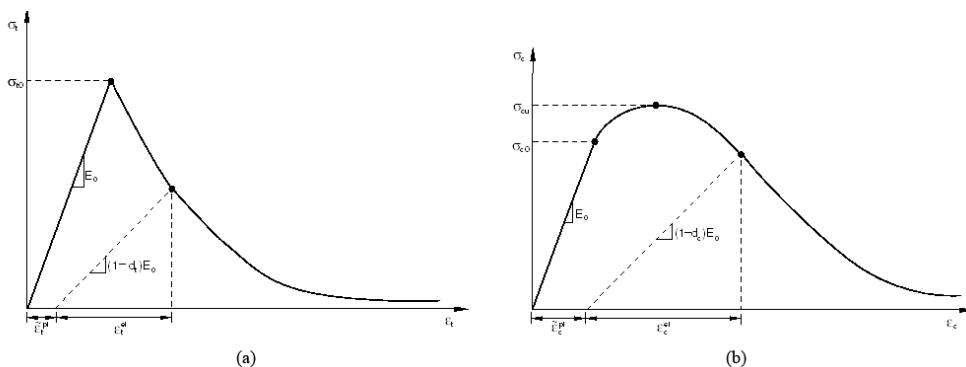


Fig. 2. (a) tensile behaviour; (b) compressive behaviour.

The model consists of a Drucker-Prager criterion modified by the introduction of a parameter K , representing the ratio between the second stress invariant of the tensile meridian and the compressive one. The constitutive model is able to describe the behavior of structures under cyclic or dynamic actions. A series of mechanical parameters have been determined in accordance with the literature (D'Altri et al., 2022) (Tab. 3). In order to couple the numerical results with the Mady's one, two distinct tensile strength values have been used. In a modeling strategy the tensile strength f_t was assumed equal to 0.44 MPa, accounted as 5% of the compressive strength. In a second case, a smaller value, equal to 0.044 MPa has been adopted, in order to compare the numerical results with the ones coming from the NT constitutive law developed in Mady. For both models tensile softening is governed by an appropriate fracture energy value calculated according to (Lourenço, 2009); in A-PLT model it has been set equal to 0.023 N/mm. Compression softening has been accounted with reference to experimental tests. Damage parameter (d_c and d_t) follow a linear law where the 90% of damage is set as the ultimate condition (Tab. 4).

Table 3. CDP additional parameters.

Ψ Dilation angle	e Eccentricity	f_{b0}/f_{c0} Biaxial strength ratio	K_c Drucker-Prager correction parameter	μ Viscosity parameter
10°	0.10	1.16	0.667	0.0001

Table 4. Tensile and compression damage of the CDP

Compression		Tension	
d_c [-]	Anelastic strain [-]	d_t [-]	Displ. [mm]
0	0	0	0
0.9	0.01	0.9	0.2

4. Comparison of results and discussion

In order to compare the different numerical results, preliminary linear dynamic analyses have been performed for all the different models, to assess their coherency in terms of modal shapes and frequencies. Then, the experimental test was simulated by setting the same boundary conditions and performing the analyses under displacement control. Fig. 3 shows the graphs of the vertical and horizontal displacement as a function of the settling displacement at the three control points (CPL, CP0 and CPR) predicted by the numerical models, and compared to the experimental results.

All the FE models provided displacements along the two components that are acceptably consistent with the experimental results. Going into more detail, observing the vertical displacement of CPL node, it appears that the experimental test exhibits an initial trend similar to the numerical ones until the formation of the crack in a mortar's joint near the basement of the left support. From this moment on, however, the left macro-element defined by the crack leads to minor displacements.

Observing the CP0 displacements, all models predict the trend observed throughout the test. Looking at the last set of the test (translation equal to 25mm), the variation of both Mady and Abaqus results with respect to the experimental data is within the 15% for the horizontal component and less than 10% for the vertical one. Generally, the outcomes of the analysis do not seem to be influenced by the complexity of the modeling strategy, as 1-d and 2-d models show reliable results. Therefore, for sake of brevity, in Fig. 4 the strain and crack details are presented solely for the 2-d models (M-PL and A-PL). The figures refer to the last steps of the analyses when the settlement reached a displacement value of 25 mm.

The comparison of the collapse mechanism evidenced by the two numerical models and the position of the actual fractures in the specimen demonstrates the reliability of the models. It is worth noting that the position of cracks in the experimental test is influenced by possible local deficiencies of the materials, a non-perfect connection of the parts or other alteration that can induce the formation of the fractures. Given the foregoing considerations, the models satisfactorily predict the plastic hinges formation and their location observed in the specimen.

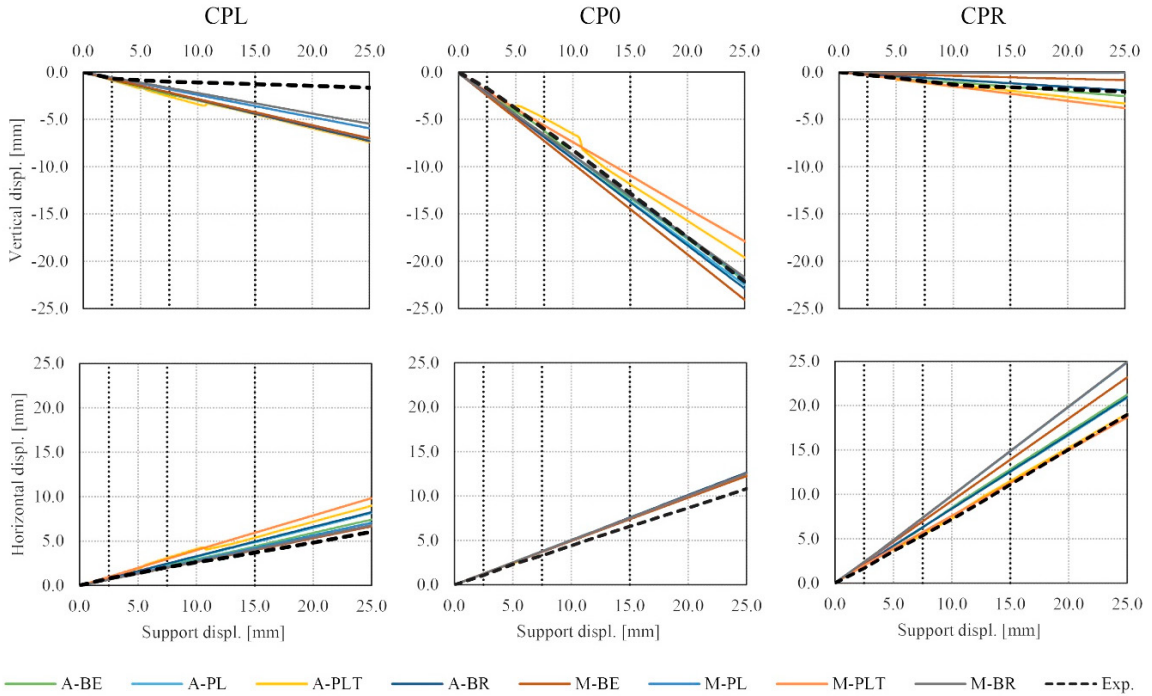


Fig. 3. Comparison in terms of displacement for the three control points according to different levels of modelling complexity.

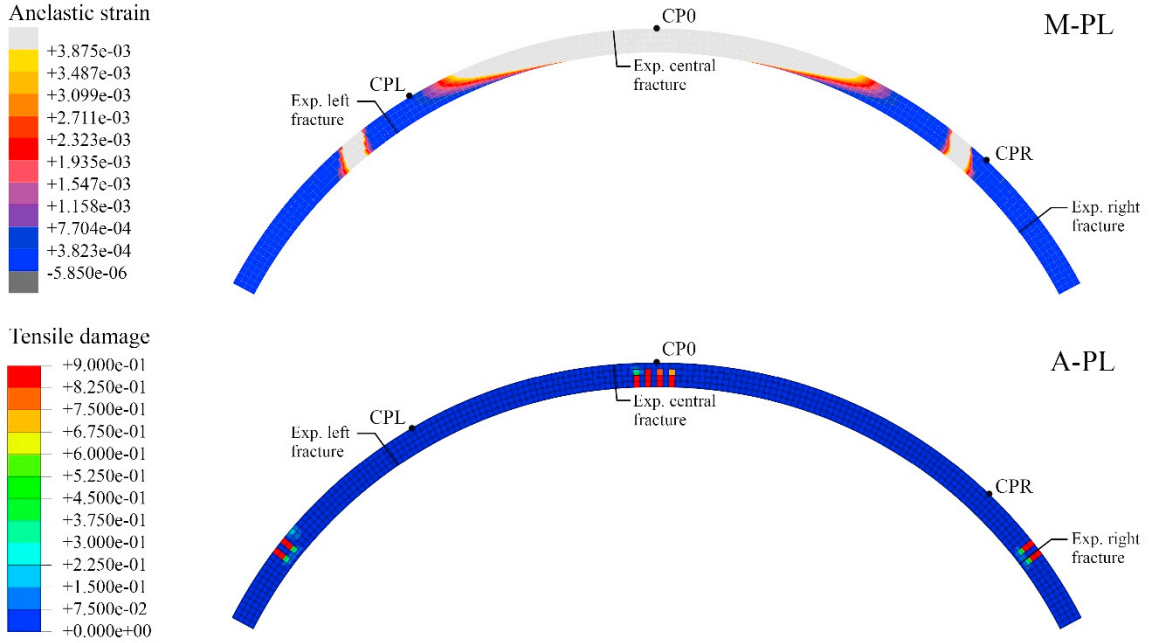


Fig. 4. Comparison between the two modelling strategies for the 2-d models in terms of anelastic strain (Mady) and tensile damage (Abaqus).

The results of this investigation have shown that the material's tensile strength is the parameter that mostly influences the crack pattern numerically evaluated. Fig. 5 shows a comparison of the damage at the left support given

by the models with a higher tensile strength (M-PLT, A-PLT) and the ones with a low or null tensile capacity (M-PL and A-PL). Although the different assumptions behind the models of the Mady and Abaqus codes, the analyses evidence the consistency of the results. In both models, the tensile capacity tends to lead the fractures in a lower position, closer to the support. On the other side, the adoption of lower values of the tensile strength leads the cracking to be placed closer to the location observed in the experimental test. The same outcome is shown in Fig. 6 by plotting the displacement of the central point (CP0). Moreover, in terms of vertical displacement, the models without tensile capacity present better agreement with respect to the experimental test. For the last settlement value, the models show variations equal to 2% and -1% for M-PL and A-PL, 19% and 12% for M-PLT and A-PLT. The trends are more similar towards the horizontal direction, where all models agree a scatter around 15%.

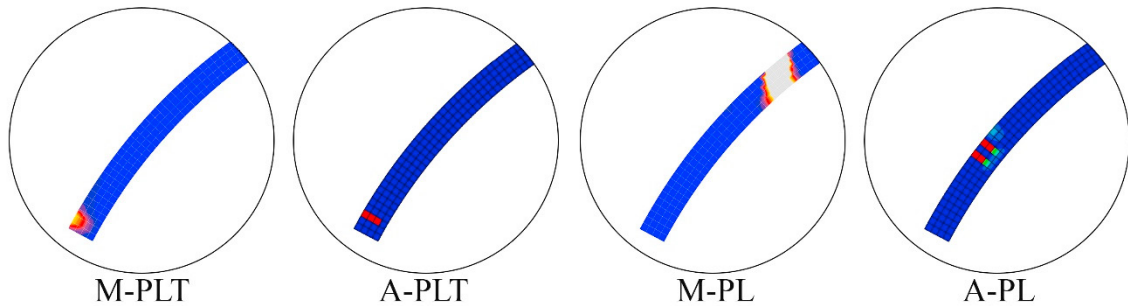


Fig. 5. Details of anelastic strain and tensile damage at the left support for PLT and PL models.

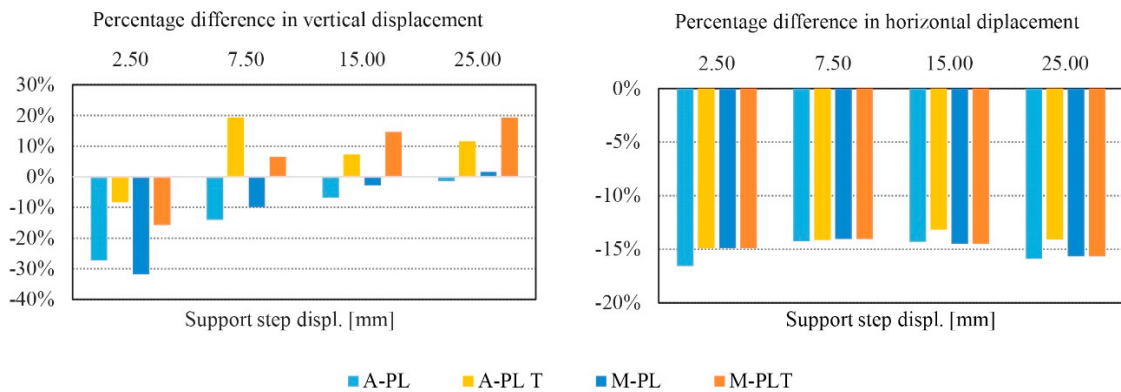


Fig. 6. Difference in percentage of vertical and horizontal displacements between developed plane models and experimental data.

5. Conclusive remarks

This paper reports the findings of a comprehensive numerical analysis performed to compare the capability of different modelling approach and constitutive laws in capturing the response of an experimental test on a masonry vault under an imposed horizontal settlement at one springing. Several FE nonlinear models have been used in the analyses, including beam, 2D and 3D models available both into the general-purpose FE code Abaqus and into the Mady code, specifically implemented to analyze the response of masonry structures.

From the results herein shown, it has been found the following conclusions: both numerical strategies allow describing the experimental behavior exhibited during the laboratory test. The comparisons in terms of displacement of the nodes show reliable outcomes for all the investigated models. Within the performed analyses, the tensile strength constitutes the key parameters that mostly affects the numerical response and the position of the plastic hinges' formation. Overall, the parameters with low or null tensile resistance leads to crack patterns more similar to the experimental results, which demonstrates the low tensile capacity of the mortar joints of the specimen. The results of

all the analytical models show consistent results. Both Mady and Abaqus models, in case of a good tensile resistance denounce a three-hinges mechanism where the rotation's formation is reached at the basis of the vault, rather than at the haunches. On the other side both A-PL and M-PL models, characterized by null / low- tensile strength, point out a higher position of the hinges, closer to the experimental one. Finally, regarding the accuracy of 1-d, 2-d and 3-d strategies, all models are able to adequately simulate the vault response. The numerical results show that simplified analyses provide suitable responses, encouraging towards the use of 1-d of 2-d models, limiting high computational efforts.

Acknowledgements

The authors acknowledge the SanMarco enterprise for offering the bricks to realize the specimen. In addition, they acknowledge Mr. Aldo Regoli from the Laboratorio Ufficiale Prove Materiale e Strutture for his support during the construction of the arch, and the student Alice Cintio for her work and support during her Master's thesis work.

References

- ABAQUS 2018. Theory and user's manuals 2018. Pawtucket (RI, USA): Hibbit, Karlsson and Sorensen.
- Como, M., 2013. Statics of Historic Masonry Constructions-Springer Series in Solid and Structural Mechanics 1, Springer-Verlag Berlin Heidelberg.
- D'Altri A. M., Cannizzaro F., Petracca M., Talledo D. A., 2022. Nonlinear modelling of the seismic response of masonry structures: Calibration strategies, *Bulletin of Earthquake Engineering*, 20, 1999-2043.
- D'Altri, A.M., Sarhosis, V., Milani, G. et al. Modeling Strategies for the Computational Analysis of Unreinforced Masonry Structures: Review and Classification. *Arch Computat Methods Eng* 27, 1153–1185 (2020). <https://doi.org/10.1007/s11831-019-09351-x>
- Engineering, 110, 87–101.
- Girardi, M., Lucchesi, M., Padovani, C., Pasquinelli, G., Pintucchi, B., Zani, N., 2012. Numerical methods for slender masonry structures: A comparative study, *Proc. of the Eleventh International Conference on Computational Structures Technology*, B.H.V. Topping, (Editor), Civil-Comp Press, Stirlingshire, Scotland, Paper 118.
- Lourenço, P. B., 2009. Recent Advances in Masonry Modelling: Micromodelling and Homogenisation. *Multiscale Modeling in Solid Mechanics*, pp. 251-294.
- Lubliner J, Oliver J, Oller S, Oñate E. A plastic-damage model for concrete. *Int J Solids Struct* 1989. doi:10.1016/0020-7683(89)90050-4.
- Lucchesi, M., Pintucchi, B., 2007. A numerical model for non-linear dynamics analysis of masonry slender structures, *European Journal of Mechanics A/Solids* 26, 88–105.
- Lucchesi, M., Pintucchi, B., Zani, N., 2018a. Masonry-like material with bounded shear stress, *Eur. J. Mech. A Solids* 72, 329–340.
- Lucchesi, M., Pintucchi, B., Zani, N., 2018b. Bounded shear stress in masonry-like bodies, *Meccanica* 53:7, 1777–1791.
- Lucchesi, M., Pintucchi, B., Zani, N., 2021a. Intersection of convex cones as stress range for plane normal elastic bodies, *Lecture Notes in Civil Engineering*, 110, 87–101.
- Lucchesi, M., Pintucchi, B., Zani, N., 2021b. Numerical methods for elastic materials with generalized stress constraints, *WIT Transactions on Engineering Sciences*, 130, 27-38.
- Milani G., Valente M., Fagone M., Rotunno T., Alessandri C., 2019. Advanced non-linear numerical modeling of masonry groin vaults of major historical importance: St John Hospital case study in Jerusalem, *Engineering Structures*, 194, 458-476.
- Pintucchi, B., N. Zani, N., 2009. Effects of material and geometric non-linearities on the collapse load of masonry arches, *European Journal of Mechanics A/Solids* 28, 45–61.
- Pintucchi, B., Zani, N., 2016. A simple model for performing nonlinear static and dynamic analyses of unreinforced and FRP-strengthened masonry arches, *European Journal of Mechanics /A Solids*, 59, 210–231.
- Seacco J., Ghiassi B., Milani G., Lourenço P. B., 2020. A fast modeling approach for numerical analysis of unreinforced and FRCM reinforced masonry walls under out-of-plane loading, *Composites Part B: Engineering*, 180, 107553.
- Zani, N., 2004. A constitutive equation and a closed-form solution for no-tension beams with limited compressive strength, *European Journal of Mechanics A/Solids* 23/3, 467–484